Synthesis and Characterization of Ion-Conducting Polymer Systems Based on EPDM Blends

H. BASHIR, A. LINARES, J. L. ACOSTA

Instituto de Ciencia y Tecnología de Polímeros del CSIC, C/Juan de la Cierva 3, 28006 Madrid, Spain

Received 6 January 2000; accepted 2 December 2000

ABSTRACT: We report on the preparation and characterization of new polymeric ionomers based on EPDM with a high norbornene content. The sulfonation level is determined by means of X-ray photoelectron spectroscopy and the microstructural characterization is obtained both through differential scanning calorimetry and dynamomechanic analysis. In addition, the effects of certain plasticizers and polymers on the microstructure of these materials were studied, as well as their conducting properties, with special attention to this latter type of behavior, in view of the interest aroused by these materials as membranes in polymer fuel cells. From the obtained results, some of the synthesized membranes can be used for fuel cells because their high conductivity ($\geq$10-2 S/cm) and their good dimensional stability (any shrinkage observed). © 2001 John Wiley & Sons, Inc. J Appl Polym Sci 82: 3133–3141, 2001

Key words: EPDM; PP; ionomers; sulfonation; XPS; DSC; DMA; complex impedance

INTRODUCTION

The severe problems deriving from air pollution, together with the difficulties and hazards implied in the use of nuclear energy, have given rise to a heated debate on the sources of energy of the future. In most fora in which the topic of energy is at stake, fuel cells are claimed to be an alternative to conventional energy generators, because of two major benefits—they can obtain high efficiency levels, and produce a minimum amount of polluting gases.[1–3]

Fuel cells are defined as a battery operating in continuous operation or else as electrochemical motors, although they are actually solid state devices that generate electricity without the aid of conventional fuels or rotating machinery (turbines, etc.). Electricity is generated as a consequence of the combination of hydrogen ions from any conventional fuel (methanol, natural gas, etc.) and oxygen atoms, following the same process operative in a car battery. The only difference is that a car battery contains its fuels internally, and, once they are consumed, they have to be replaced recharging the battery, whereas the fuel cell is equipped with a device (reformer) that supplies fuel continually. Thus, a fuel cell is able to operate in the continuous mode, while there is a fuel supply and does not have to be recharged periodically.

In addition to the benefit of being able to produce fuel cells with the desired power output stacking the necessary units serially or parallel, there are other advantages worth highlighting, such as their considerable environmental acceptability, i.e., CO_2 emissions are already limited to the utmost at present, but for the year 2000 new plants are in the project phase whose CO_2 emissions will not surpass 0.6 MMT equivalent carbons. Fuel cells have a low noise emission: 60

Correspondence to: J. L. Acosta (ictal02@fresno.csic.es).

Contract grant sponsor: The CE (within the frame of the Non Nuclear Energy R and D Program); contract grant number: JOE2-CT97-0049.

Journal of Applied Polymer Science, Vol. 82, 3133–3141 (2001)

decibels. They are designed with nil water consumption: they will re-utilize the water produced by their own electrochemical reaction. They achieve a high level of efficiency, i.e., depending on the type of battery, the efficiency range moves between 40 and 60% and is not affected by the Carnot cycle. When the byproducts from electrochemical reaction are exploited, efficiency surpasses 85%. Fuel cells are modular constructs, which means that plants can be given a modular configuration. A great variety of fuels can be used. The prime fuel source was hydrogen, which can be obtained from natural gas, pit coal gas, methanol, and from many hydrocarbons. Last but not least, fuel cells possess a high potential of cogenerating other products, such as steam, which can be given a practical application.

As a function of the electrolyte used, fuel cells receive different names. For instance, if they have a high proton-conducting polymer membrane, they are known as polymeric fuel cells, and their main application is in electrical cars. Two of the major problems to be overcome in the field of polymeric membranes to ensure adequate marketing[4–6] are: (a) lowering the presently high price of commercial membranes and (b) eliminating the Fluor from these commercial membranes for environmental reasons, i.e., to the purpose of facilitating their treatment within current urban and industrial waste procedures.

Thus, it is the ultimate aim of this research to obtain new polymer membranes with a high proton-conducting potential (according to the specialized literature, the conductivity must rise approximately 10^{-2}/cm), and high chemical and dimensional stability [any shrinkage at the operating temperature (100°C) of fuel cells]. To this effect, we have synthesized different protonic conductors through controlled sulfonation of EPDM, incorporating polypropylene (PP) or pure EPDM, as well as several plasticizers, in order to favor membrane processing. In this work, the effect exerted by pure polymers and plasticizers on the microstructure and the electrical properties of the membranes obtained is described and analyzed.

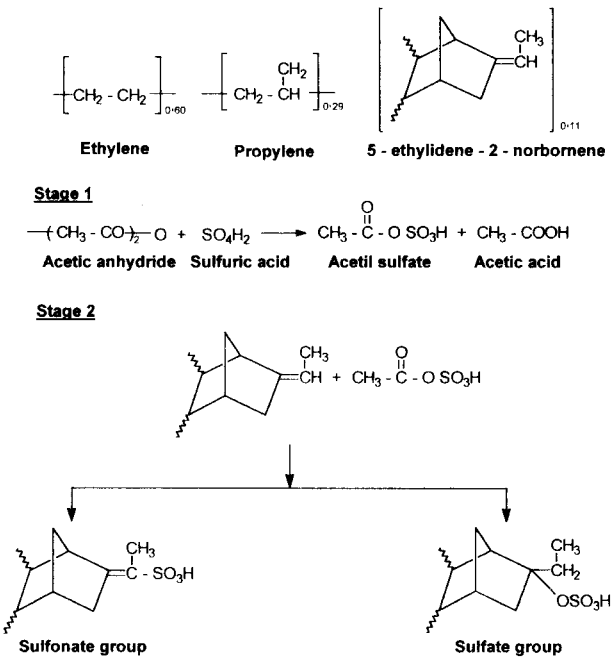

Figure 1 Sulfonation mechanism of EPDM.

EXPERIMENTAL

EPDM Vistalan 9500 (contains 60 wt % ethylene, 29 wt % propylene, and 11 wt % 5-ethylidine-2-norbornene) supplied by Exxon Chemical

Table I Binding Energies of C 1s and S 2p, Atomic Relations, and Sulfonation Level of Sulfonated EPDM

Samples	Acetyl Sulfate Concentration (mol)	C 1s (eV)	S 2p (eV)	S/C (Atoms)	—SO_3H (%)
EPDM-I	1	284.9 (76)			
		286.1 (24)	169.4	0.010	3.06
EPDM-II	2	284.9 (76)			
		286.0 (24)	168.7	0.008	2.48
EPDM-III	3	284.9 (89)			
		286.2 (11)	169.1	0.016	4.90
EPDM-IV	4	284.9 (80)			
		286.1 (20)	169.2	0.018	5.51

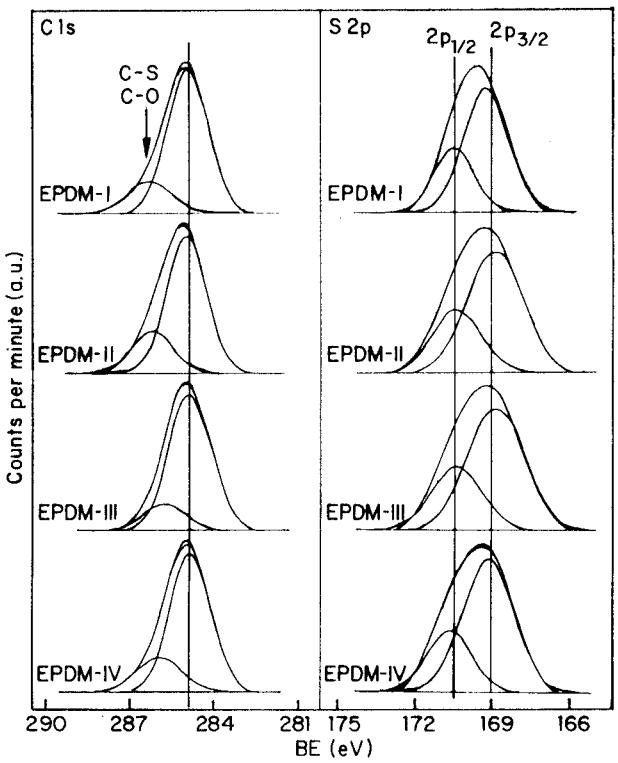

Figure 2 Photoelectron spectra of the samples.

(France); acetic anhydride and hexane were supplied by Panreac as was sulphuric acid; paraffin oil (Repsol) and butyl pftalate (Jaber) were used without previous purification; deionized water was milli-Q quality.

Thermoplastic EPDM was sulfonated using the procedure described by Makowski: acetic anhydride and concentrated sulphuric acid were added slowly with vigorous stirring to a solution of EPDM in hexane so that the temperature did not exceed 0°C; after 30 min, the reaction was concluded by adding ethanol. The acid form of the sulfonated EPDM was isolated by steam stripping, a process in which the polymer reaction is added to hot deionized water and the hydrocarbon solvent is flashed off leaving a water-wet polymer crumb, which is washed several times until neutral pH and finally dried at 100°C.

Blends of the components were obtained from the melt in a Brabender torque rheometer using a thermoplastic mixing chamber (type W60) preheated to 473 K. The rotor speed was set at 55 rev min^{-1} and the materials remained in the chamber for about 10 min once the torque had stabilized, which ensured perfect homogenization.

Membranes of suitable thickness were manufactured by compression in a Collins hydraulic press heated at 200°C for 10 min and then cooled under press until room temperature.

The salt form of the sulfonated EPDM were converted to their acid form by means of strong acids; membranes were immersed in a 50°C diluted watery solution of a strong acid for several hours.

Photoelectron spectra were acquired with a VG ESCALAB 200R spectrometer provided with MgKa radiation (hv = 1253.6 eV) and a hemispherical electron analyser. The spectrometer was calibrated using the Cu 2p3/2 and the Au 4f7/2 peaks of a metallic sample. The C ls, S 2p, and O ls core-level spectra were recorded in kinetic energy ranges at a pass energy of 20 eV. Each spectral region was scanned between 40 and 100 times, depending on the intensity of the signal, in order to get an acceptable signal-to-noise ratio at reasonable acquisition times. Radiation damage has been considered negligible, considering the agreement between spectra recorded after X-ray exposure of the sample at 5 min and 200 min. The curve-resolving procedure involved the fitting of the experimental curve to Gaussian/Lorentzian mix of variable proportion, the estimated error of fit being ±7%, the goodness-of-fit

Table II DSC and DMA Analyses of the Samples

	Sulfonation of EPDM		DSC		DMA
Samples	Norbornene Unit (mol)	Acetyl Sulfate (mol)	T_g (°C)	C_p (J/K)	T'_g (°C)
EPDM-SH-I	1	1	−43.0	0.43	−45.4
EPDM-SH-II	1	2	−43.0	0.47	−42.6
EPDM-SH-III	1	3	−44.4	0.41	−41.4
EPDM-SH-IV	1	4	−38.6	0.72	−35.8

Table III DSC and DMA Analyses of the Samples

	Composition					DSC		DMA
Samples	EPDM-SH (wt %)	PP (wt %)	EPDM (wt %)	Paraffin Oil (wt %)	Butyl Phthalate (wt %)	T_g (°C)	C_p (J/K)	T'_g (°C)
BL-1	90	10	—	—	—	−40.2	0.26	−40.3
BL-3	90	—	10	—	—	−40.3	0.40	−41.6
BL-5	90	—	—	10	—	−42.9	0.34	−45.9
BL-6	90	—	—	—	10	−38.6	0.66	−42.8

was estimated from χ^2 values. The error in kinetic energy was estimated to be ±0.1 eV. The conversion from Ek to Eb (binding energy) scales was computed by considering the maximum of the C 1s peak, corresponding (arbitrary) to 284.9 ± 0.1 eV, as being characteristic of organic carbon. The flat films were fixed on a long rod placed in the turbo-pumped pretreatment chamber of the spectrometer and outgassed at 10^{-6} Torr before being moved into the analysis chamber in which the base pressure was maintained below 3×10^{-9} Torr during data acquisition.

Glass transition temperatures (T_g) were measured using a Mettler TA 40000 differential scanning calorimeter. Samples were melted at 353 K for 10 min to avoid any previous thermal history, and then rapidly quenched using liquid nitrogen. Thermograms were then recorded at a heating rate of 5°C/min.

Non-isothermal crystallization was followed also on a Mettler TA3000 differential scanning calorimeter. Samples were heated at 373 K, held there for 10 min, and then cooled at different cooling rates; the crystallization endotherms were recorded over the cooling cycle.

Dynamic mechanical measurements were conducted with a 983 Dynamic Mechanical Analyser TA Instrument at 3, 10, and 30 Hz in the temperature range of 133 ~ 413 K and at a rate of 2 K min^{-1}.

Conductivity measurements were performed by using a Hewlett-Packard Model 4192A impedance analyser coupled to a computer, in the frequency range of 10^{-2} to 10^4 kHz at room temperature.

RESULTS AND DISCUSSION

EPDM sulfonation occurs through double bonding of the norbornene units, according to the mechanism described in Figure 1. This type of reaction may give rise to two different groups: on the one hand, the sulfonic group (—SO_3H) responsible for protonic conductivity and, on the other hand, the sulfate group (—OSO_3H) lacking conductivity and obtained, as a general rule, in the presence of water. Under the experimental conditions, however, it proved impossible to detect the sulfate group with any type of spectroscopy, including X-ray photoelectron spectroscopy. This legitimates us to discard sulfate group formation under the experimental conditions, which are described in the experimental part of this work.

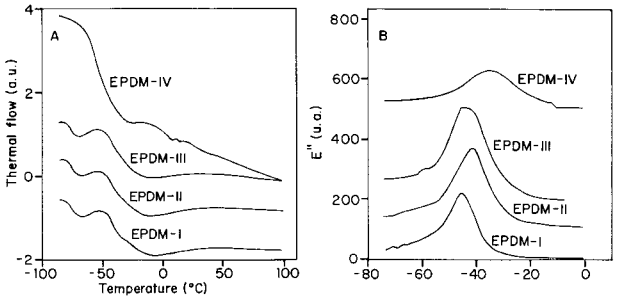

Figure 3 (A) DSC and (B) DMA analyses of the samples.

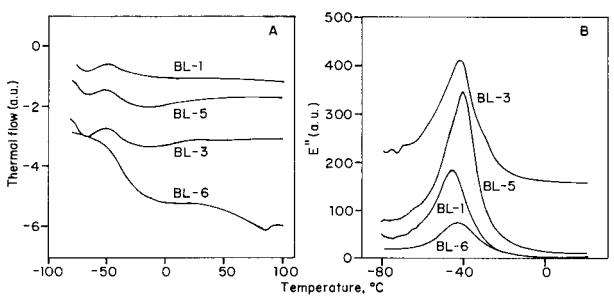

Figure 4 (A) DSC and (B) DMA analyses of the samples.

Table IV DSC and DMA Analyses of the Samples

	Composition			DSC		DMA
Samples	EPDM-SK (wt %)	EPDM-SZn (wt %)	PP (wt %)	T_g (°C)	C_p (J/K)	T'_g (°C)
SL-1	100	—	—	−41.4	0.66	−36.1
SL-7	80	—	20	−40.2	0.14	−40.5
SL-3	—	100	—	−41.3	0.78	−36.2
SL-9	—	80	20	−41.3	0.52	−37.7

The analytic data obtained from X-ray photoelectron spectroscopy for all EPDM samples sulfonated with different amounts of reagent allowed us to assess the sulfonation level through sulphur content (S) determination. Table I lists the binding energies of C 1s and S 2p, as well as the atomic S/C ratios and the sulfonation percentage (SO_3H) reached in each sample. The respective spectra yielding these values are compiled in Figure 2.

The sulphur atoms from the —SO_3H group could be deconvoluted into two contributions (S $2p_{3/2}$ and S $2p_{1/2}$), as the resolution of the instrument allowed for such breakdown. But there is only one species, i.e., the one corresponding to the sulfonic group (—SO_3H), as shown in Figure 1. The carbon (C 1s) is asymmetric (Fig. 2), thus yielding two components: one at 284 eV which comprises the C—C, C═C, and C—H bonds whose binding energies are so close that they cannot be resolved, and a second component around 286.1 eV referring to C—O and C—S bonds, mostly C—O bonds which are fundamentally attributable to pollution through cleaning alcohol and other agents.

The sulfonation level of the samples is determined from the S/C ratios in Table I. The percentage expressed in the Table corresponds to the percentage of monomeric units contained in the sulfonic group in the EPDM, concretely speaking, the percentage of norbornene units in which sulfonation has occurred vis-à-vis the other units (ethylene, propylene, and unsulfonated norbornene). As can be observed, as a function of increasing sulfonant concentration in the medium the sulfonation level rises, except for sample EPDM-II, whose abnormally low level may be attributed to experimental error. The maximum sulfonation level reached under the experimental conditions chosen is approximately 50% of the potential absolute maximum.

All of the samples were subjected to microstructural analysis by means of T_g determination through two different techniques, i.e., differential scanning calorimetry (DSC) and dynamo-mechanic analysis (DMA). The results obtained with one and the other instrumental technique are compiled in Tables II and III, and Figures 3 and 4 show some sample plots of the results discussed.

Table V Kinetic Parameters of the Non-Isothermal Crystallization of the Samples

	Composition (wt %)			β		
Samples	EPDM-SK	EPDM-SZn	PP	(°C/min)	n	Log K
SL-06	80	—	20	6	3.9	−1.6035
				8	3.9	−1.2895
				10	3.5	−0.6869
				12	3.1	−0.3666
SL-09	—	80	20	6	5.0	−1.4836
				8	4.9	−1.0021
				10	4.7	−0.8552
				12	4.4	−0.3174

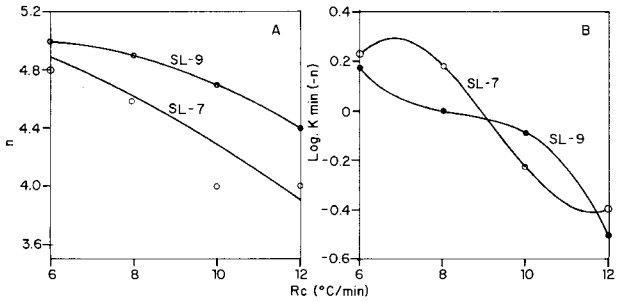

Figure 5 Effect of the crystallization rate on the kinetic parameters of the samples

The effect of sulfonic group (—SO_3H) concentration on the T_g of pure EPDM is shown in Figure 3, which contrasts the thermograms recorded by means of DSC with the dynamo-mechanic spectra of the four samples sulfonated at four different sulfonate concentrations and constant reaction time. DSC of the samples allows detection of T_g, with some inaccuracies, however. Nevertheless, a general trend toward a rise of T_g as a function of increasing sulfonic group concentration in the ionomer (Table II) is clearly perceptible. In contrast, dynamo-mechanic spectroscopy confirms this trend with absolute accuracy. As expected, the increment of sulfonic groups translates into a rise in T_g, as a consequence of the extraordinarily polar nature of this cluster. The interaction force is so strong that it raises the T_g by up to 10°C above that of the less intensely sulfonated samples.

When PP or the unsulfonated polymer itself or else some plasticizers are incorporated into the sulfonated sample EPDM-III, the scenario changes radically. As could be expected, the strong intermolecular forces of the sulfonic groups are canceled out or damped, and the typical behavior of conventional, plasticizers-filled polymer systems comes to light, i.e., T_g drops to lower temperature ranges, as a consequence of the internal lubricating effect among the polymer chains.

In Figure 4, the DSC thermograms are contrasted with the dynamo-mechanic spectra of the different ionomers obtained from the EPDM blends sulfonated with PP, EPDM, or the two plasticizers. As usual, thermal analysis shows a clear downward shift trend of the T_g [Fig. 4(A)], a trend which is totally confirmed when analyzing the dynamo-mechanic data [Fig. 4(B)], which demonstrate that low unsulfonated PP or EPDM concentrations or the presence of low butyl phthalate or paraffin oil concentrations are able to cause the T_g of EPDM to shift toward lower temperatures, the most important drop being observed for paraffin oil, achieving a downward shift of almost 5°C. This behavior has two beneficial effects on the resulting material: the manufacture of membranes becomes technologically easier, and its dimensional stability is remarkably enhanced.

From a thermal point of view, the sulfonic group is fairly unstable, hence demanding for protective agents, which are provided by means of the formation of the respective potassium or zinc salts. In this research, we obtained the potassium and zinc salts from sulfonated EPDM. It is noteworthy that one of the most relevant characteristics of these materials relates to their inability to form membranes. This is the reason that they have to be incorporated into a polymer of high thermal and dimensional stability (PP) to make membrane manufacture feasible. However, to reestablish their ion conductivity, it is necessary to regenerate the sulfonic group by means of heterogeneous reactions with strong inorganic acids.

On these lines, the samples were obtained whose compositions are compiled in Table IV, and from them the effects were determined exerted by the potassium or zinc salts on the amorphous and crystalline structures of PP. To this end, the re-

Table VI Effect of the Hydration Time on the Conductivity of the Samples

Samples	Hydration 50°C (h)	Conductivity (σ) 25°C S · cm^{-1} 1	2
EPDM-SH-I	0	—	—
	3	—	—
	6	—	—
	24	2E-8	5E-9
EPDM-SH-II	0	—	2E-7
	3	6E-7	5E-6
	6	5E-7	5E-5
	24	2E-7	2E-5
EPDM-SH-III	0	2E-7	4E-7
	3	2E-5	6E-6
	6	5E-5	6E-5
	24	2E-2	1E-3
EPDM-SH-IV	0	3E-8	2E-7
	3	1E-4	9E-5
	6	1E-4	4E-4
	24	6E-4	6E-4

Table VII Effect of the Hydration Time on the Conductivity of the Samples

Samples	Composition					Hydration 50°C (h)	Conductivity (σ) 25°C $S \cdot cm^{-1}$	
	EPDM-SH-III (wt %)	PP (wt %)	EPDM (wt %)	Paraffin Oil (wt %)	Butyl Phthalate (wt %)		1	2
BL-1	90	10				0	—	—
						3	—	—
						6	—	—
						24	—	—
BL-3	90		10	—	—	0	8E-7	1E-7
						3	5E-5	2E-6
						6	6E-5	1E-5
						24	2E-3	8E-3
BL-5	90		—	10	—	0	2E-8	4E-7
						3	3E-6	6E-7
						6	3E-6	5E-5
						24	9E-4	8E-4
BL-6	90			—	10	0	3E-7	4E-5
						3	2E-6	3E-6
						6	5E-6	8E-6
						24	8E-5	2E-5

spective T_gs were obtained through DSC, the results of which are compiled in Table IV, as well as the respective non-isothermal crystallization kinetics, whose most important data will be discussed below.

The kinetics of isothermal crystallization were analyzed by means of the Avrami equation[7]:

$$(1 - \chi_t) = \exp(-Kt^n)$$

where n is the Avrami exponent, a numerical value that provides information about the type of nucleation and the crystal growth geometry, and K is the rate constant. The plot of $\log\{-\ln[1 - X(T)]\}$ against $\log t$ yields straight lines for each cooling rate β by conversions below 30%.

Table V summarizes the relevant data obtained for the different experimental cooling rates (β), and in Figure 5, the effects of the cooling rates on the kinetic parameters (crystal growth geometry) are shown, as well as the rate constant.

The growth geometry of the crystalline structure of PP is strongly influenced by the presence of one or the other salt, Avrami's exponent n is much higher in the case of zinc than potassium, which is indicative of the fact that in each case, a different spherulitic growth mechanism is involved, which proves to be independent of the cooling rate applied. As was to be expected, the crystallization rate diminishes proportionate to the increase in the cooling rate, in our case independent of the salt present in the sample.

The electrical characterization was conducted by means of complex impedance spectroscopy on samples of the different families hydrated in deionized water at 50°C for periods of time between 1 and 24 h. For each sample, two different measurements were implemented on different sample units, in order to demonstrate the reproducibility of the measurements. The results obtained at the different experimental hydration times (Ht) are exhaustively compiled in Tables VI and VIII. In Figure 6, the complex impedance analyses are shown of the different sulfonated EPDM membranes, together with the complex impedance diagrams of sample EPDM-SH-III obtained at several hydration times. The general trend to be highlighted is that sample conductivity (obtained from the y-intersect of the semicircle) increases proportionate to the increase in hydration time. In more accurate terms, Figure 6(B) presents the effect exerted by the hydration time on the EPDM samples with varying sulfonation degrees. The samples prove, logically, their conductivity to increase as a function of hydration time. Nevertheless, the sample labeled EPDM-SH-III ($[SO_3H] = 4.9$) achieves the highest level of conductivity, despite the fact that it is not the

Table VIII Effect of the Hydration Time on the Conductivity of the Samples

Samples	Composition EPDM-SK (wt %)	Composition EPDM-SZn (wt %)	Composition PP (wt %)	Hydration 50°C (h)	Conductivity (σ) 25°C S · cm^{-1} 1	Conductivity (σ) 25°C S · cm^{-1} 2
SL-1	100	—	—	0	6E-8	1E-7
				3	6E-3	2E-3
				6	1E-2	1E-2
				24	4E-2	1E-2
SL-7	80	—	20	0	2E-6	5E-7
				3	5E-4	2E-4
				6	6E-4	8E-5
				24	5E-5	6E-6
SL-3	—	100		0	8E-9	6E-9
				3	9E-5	6E-5
				6	1E-5	1E-5
				24	3E-4	3E-5
SL-9	—	80	20	0	7E-9	6E-9
				3	1E-6	2E-5
				6	2E-7	1E-6
				24	9E-7	6E-6

sample containing the highest sulfonation level, which is the sample labeled EPDM-SH-IV ([SO_3H] = 5.5). The reason for this behavior has to be sought in the strong ionic interactions that trigger the SO_3H groups between the polymer chains, interactions which give rise to different aggregate states, extending from isolated ionic pairs (low SO_3H group concentrations) up to multipletes or clusters (higher SO_3H group concentrations), thus causing polymer chain movement constraints, which, in the case of ionomers, translate into a water or ion throughput difficulty. According to the data obtained in this research, sulfonic group concentrations above 5% in the blend favor cluster formation in the membrane, which inhibits the penetration of water into the polymer backbone and hence proton movement through the membranes is hindered, which considerably diminishes conductivity.

When small amounts (10%) of PP are incorporated into the EPDM-SH-III sample, or else of the unsulfonated polymer itself or of the experimental plasticizers (Table VIII), there occur minor changes [Fig. 7(B)]. With the incorporation of 10% EPDM, membranes are obtained that possess better hydrating properties than those of the pure polymers. This is demonstrated by the fact that a higher conductivity is reached. Under the same concentration conditions, butyl phthalate reaches a conductivity that is 100 times lower. Paraffin oil incorporated into EPDM-SH-III presents an intermediate behavior, as compared with the previously stated cases. It should be stressed that low

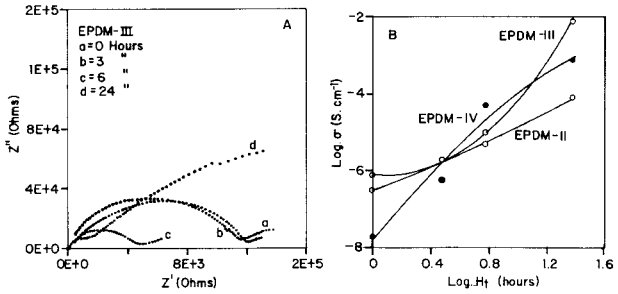

Figure 6 (A) Effect of the hydration time on the complex impedance spectra of EPDM-SH, and (B) effect of the hydration time on the conductivity of the samples.

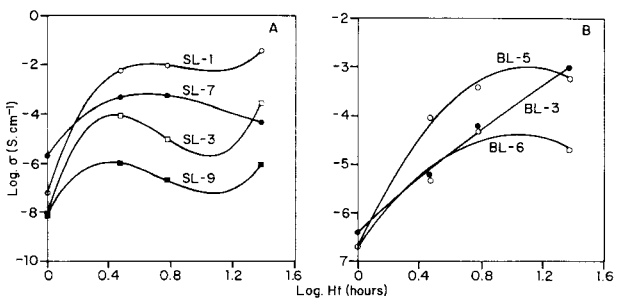

Figure 7 Effect of the hydration time on the conductivity of the samples.

PP concentrations added to sulfonated EPDM favors membrane manufacture, but inhibits water penetration so that the membranes are void of conductivity.

In terms of equivalent circuits, all of these materials react to one and the same type of circuit, comprising a resistance and a condenser in parallel and a constant phase element placed serially.

CONCLUSIONS

The conventional plasticizers used in this study (butyl phthalate or paraffin oil) provide the membrane with better processing properties and dimensional stability, although conductivity is impaired, because of deficient hydration and swelling properties of the membranes. When PP is incorporated, the opposite effect is produced, regarding the influence exerted on EPDM.

REFERENCES

1. LaConti, A. B.; Fragala, A. R.; Boyack, J. R. Proceedings of the Symposium on Electrode Materials and Processes for Energy Conversion Storage. McIntyre, D. E.; Srinivasan, S.; Will, F. G. De., PV 77-6, The Electrochemical Society Proceedings Series, Princeton, New Jersey, 1977, p. 354.
2. Kesting, R. E. Synthetic Polymeric Membranes; John Wiley & Sons: New York, 1985.
3. Bockris, J. O'M; Srinivasan, S. Fuel Cells: Their Electrochemistry; McGraw-Hill: New York, 1969.
4. Lemmons, R. J. J Power Sources 1990, 29, 251.
5. Strasser, K. J Power Sources 1992, 37, 209.
6. Prater, K. B. J Power Sources 1992, 37, 181.
7. Avrami, M. J. J Chem Phys 1938, 7, 1103.